



Cryospheric Monitoring and Research by Means of ERS

Helmut Rott ¹, Thomas Nagler ², Wolfgang Rack ³

¹ *Institut für Meteorologie und Geophysik, Universität Innsbruck, Innrain 52, A-6020 Innsbruck*

² *Institut für Meteorologie und Geophysik, Universität Innsbruck, Innrain 52, A-6020 Innsbruck*

³ *Institut für Meteorologie und Geophysik, Universität Innsbruck, Innrain 52, A-6020 Innsbruck*

VGI – Österreichische Zeitschrift für Vermessung und Geoinformation **84** (2), S. 151–156

1996

Bib_TE_X:

```
@ARTICLE{Rott_VGI_199626,  
Title = {Cryospheric Monitoring and Research by Means of ERS},  
Author = {Rott, Helmut and Nagler, Thomas and Rack, Wolfgang},  
Journal = {VGI -- {"0}sterreichische Zeitschrift f{"u}r Vermessung und  
Geoinformation},  
Pages = {151--156},  
Number = {2},  
Year = {1996},  
Volume = {84}  
}
```



tion: Application to an Antarctic Ice Stream. *Science*, vol. 262, pp. 1525-1530, Dec. 1993.

- [6] *L.C. Graham*: Synthetic interferometric radar for topographic mapping. *Proceedings of the IEEE*, vol. 62, pp. 763-768, June 1974.
- [7] *J.R. Joughin, D.P. Winebrenner and M.A. Fahnestock*: Observations of ice-sheet motion in Greenland using satellite radar interferometry. *Geophysical Research Letters*, vol. 22, pp. 571-574, Mar. 1995.
- [8] *D. Massonnet, M. Rossi, C. Carmona, F. Adragna, G. Peltzer, K. Feigl and T. Rabaute*: The displacement field of the Landers earthquake mapped by radar interferometry. *Nature*, vol. 364, pp. 138-142, July 1993.

[8] *E. Rignot, K.C. Jezek and H.G. Sohn*: Ice Flow Dynamics of the Greenland Ice Sheet from SAR Interferometry. *Geophysical Research Letters*, vol. 22, pp. 575-578, Mar. 1995.

[9] *H.A. Zebker and R.M. Goldstein*: Topographic mapping from interferometric Synthetic Aperture Radar Observations. *Journal of Geophysical Research*, vol. 91, pp. 4993-4999, Apr. 10, 1986.

Anschrift der Autoren:

Dipl.-Ing. Heinrich Frick, Dipl.-Ing. Rainer Kalliany, Institut für Computerunterstützte Geometrie und Graphik, TU Graz, Münzgrabenstraße 11, A-8010 Graz.



Cryospheric Monitoring and Research by Means of ERS

Helmut Rott, Thomas Nagler and Wolfgang Rack, Innsbruck

Zusammenfassung

Im Rahmen von Experimenten betreffend die Nutzung des Aktiven Mikrowellen Instrumentes (AMI) der Europäischen Erdbeobachtungssatelliten ERS-1 und ERS-2 wurden Methoden und Anwendungen auf dem Gebiet der Kryosphärenforschung untersucht. Feldmessungen der Radarrückstreuung in den Alpen und in der Antarktis lieferten Grundlagen für die Analyse der Satellitendaten. Mittels AMI Scatterometer Daten wurden großflächig Eigenschaften von Schnee und Eis über der Antarktis untersucht. Es wurde ein Verfahren zur Kartierung schmelzenden Schnees mittels AMI Synthetisch Apertur Radar (SAR) entwickelt, das bereits für die Modellierung von Schnee- und Gletscherschmelze erprobt wurde. ERS-1 SAR Daten der Antarktischen Halbinsel und des Südlichen Patagonischen Eisfeldes zeigten einen markanten Rückzug des Eises, was als Hinweis auf regionale Klimaänderungen zu sehen ist.

Abstract

In the frame of scientific experiments on the use of the Active Microwave Instrument (AMI) of the European Earth Observation Satellites ERS-1 and ERS-2 methods and applications for snow and ice monitoring have been investigated. Ground based scatterometer measurements and field campaigns in the Alps and in Antarctica provided the basis for the analysis of the spaceborne microwave data. Large scale characteristics of Antarctic snow and ice were analyzed by means of AMI scatterometer data. An algorithm was developed for snow mapping by means of AMI Synthetic Aperture Radar (SAR) and successfully tested for modelling of snow and glacier melt. Dramatic changes of ice extent, including the collapse of an ice shelf, have been detected by means of ERS-1 SAR on the Antarctic Peninsula and on the Southern Patagonian Icefield, providing evidence for regional climatic change.

1. Introduction

ERS-1, the first European Remote Sensing Satellite, was launched by the European Space Agency (ESA) on 17 July 1991, followed by its successor ERS-2, launched on 20 April 1995. Though the sensors had been designed for research and applications in coastal zones, in polar regions, and for global ocean processes, in the course of the ERS-1 mission a wide range of applications developed also over land surfaces [1].

In the frame of three scientific ESA-approved experiments with ERS-1 and ERS-2 (Principal In-

vestigator H. Rott) scientists of the University of Innsbruck have been involved in the development of methods on the use of ERS data for snow and ice monitoring and research and studied dynamics and ice/climate interactions on Alpine glaciers, on the Patagonian Icefield and in various parts of Antarctica. Research on scattering signatures provided the basis for the analysis of satellite data. The main activities were related to the Active Microwave Instrument (AMI) of ERS.

AMI operates in the C-band at 5.3 GHz (5.6 cm wavelength) parallel (VV) polarizations; it comprises a synthetic aperture radar (SAR) with high

spatial resolution (20 m×25 m with 3 azimuth looks) and 100 km swath width, and a scatterometer with about 50 km spatial resolution and 500 km swath width. These two instruments can operate only alternately. The SAR is a high resolution all weather imaging sensor, whereas the scatterometer, though designed to measure wind velocity and direction at the ocean surface, has found to be useful also for a range of large-scale land applications, including snow and ice monitoring.

2. Backscattering Signatures of Snow and Ice

For the analysis of spaceborne microwave data it is necessary to know about the interaction mechanisms of the microwaves with the targets of interest. Backscattering and emission of snow and ice at 5 GHz and 10 GHz were measured with a scatterometer/radiometer at various sites in the Alps and during two field expeditions in different parts of Antarctica [2]. In addition, data from calibrated spaceborne or airborne sensors were utilized for signature research in combination with field measurements of the physical properties of the observed targets [2, 3]. Liquid water content, grain size, stratification, and surface roughness are the key parameters for microwave scattering.

Fig. 1 shows examples of characteristic backscattering signatures. The angular dependence of the backscattering cross section σ° at 5.3 GHz for co-polarized and cross-polarized antennas was measured with the field scatterometer over a meadow near Innsbruck under snow-free conditions and for wet snow cover. The penetration of the microwaves in wet snow is few centimeters only. Due to the high dielectric losses and the comparatively smooth surface, σ° of the wet snowpack is several dB lower than σ° of the snow-free meadow. The contrast of wet snow versus targets with rough surfaces is even higher, as evident in Fig. 1 for rock and moraine surfaces. The σ° - curve for these targets is based on an analysis of ERS-1 SAR data over the Alpine test area Ötztal using digital elevation data to calculate the local incidence angle of the radar beam. The SAR-based algorithms for wet snow cover monitoring are utilizing this contrast in σ° . The σ° -differences are highest for cross-polarized σ° , indicating the high capability for mapping wet snow. Presently, cross-polarized channels are available only on airborne SAR systems and had been operating in space during short-term shuttle radar experiments.

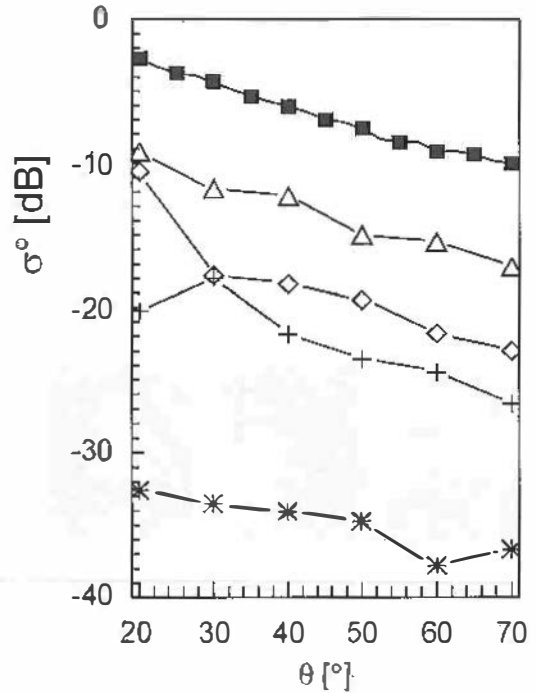


Fig. 1: Radar cross section σ° at 5.3 GHz in decibels, as function of the incidence angle θ of the radar beam. Co-polarized σ° : Δ snow-free meadow, \diamond wet snow, measured with a ground-based scatterometer; \blacksquare bare soil and rock, based on ERS-1 SAR measurements. Cross-polarized σ° : + snow-free meadow, * wet snow.

Whereas wet snow can be clearly identified in C- and X-band SAR imagery, the dielectric losses in dry snow are small. This means that the main part of radar signal is able to reach the ground below a dry winter snowpack, and the observed radar signal is dominated by scattering at the snow/ground interface. For this reason σ° is similar for a surface if it is free of snow or covered by dry snow. For the examples in Fig. 1, σ° for dry winter snow differs by 2 dB at maximum from the corresponding snow-free curve.

3. ERS-1 Scatterometry Over Antarctica

In order to learn about the spatial distribution of the different snow and ice regimes, backscattering characteristics have been investigated over Antarctica by means of ERS-1 AMI in scatterometer mode. Ground based scatterometer measurements and related studies of snow and ice properties, carried out during two field expeditions in different parts of Antarctica, assisted in the understanding of the ERS-1 data. Three parameters were identified which characterize

the different regimes of polar firn: the mean intensity, the incidence angle gradient, and the azimuthal anisotropy [4, 5]. These parameters depend on the snow metamorphic state which is related to accumulation rate, temperature, and wind.

Over the interior parts of Antarctica, where the snow is permanently dry, σ° was found to be very stable in time, enabling sensor intercalibrations and monitoring of sensor stability. Dry snow in the accumulation zones of glaciers and ice sheets shows comparatively high backscattering because the dielectric losses are low and the signal is integrated over many layers. Highest σ° is observed for refrozen firn along the coast in winter due to scattering at ice layers and ice lenses originating from summer melt events. In the katabatic wind zones σ° shows strong variations with the azimuth angle. This anisotropy, which in extreme cases results in ocean-like backscattering behaviour, is related to the intensity and direction of the dominating wind.

Along the coast and on the Antarctic Peninsula the temporal variations of backscattering signatures provide information on areal extent and duration of surface and sub-surface melt. As an example, Fig. 2 shows the time sequence of σ° for an area of about 100 km x 100 km size on Larsen Ice Shelf, about 200 km south of the area shown in the SAR image (Fig. 4). When melting starts around November 20, σ° drops from 0 dB for the frozen firn to values around -20 dB in mid-December, indicating wet snow with liquid water content of several per cent. During short freezing events between mid-December and mid-March σ° increases temporarily by a few dB, the main part of the firn below the frozen crust remains wet. After mid-March σ°

approaches asymptotically the winter value for completely frozen firn. This information on summer melt is of considerable interest for studies of climate and mass balance in Greenland and on the Antarctic Peninsula.

4. The SAR Snow Mapping Algorithm

The areal extent of the snowpack is a key parameter for modelling and forecasting snow-melt runoff and for climate research. Though in general dry snow can not be detected by SAR, time sequences of SAR images provide information on temporal dynamics of melting snow which is of high interest for water management and hydrology.

An algorithm for mapping melting snow in mountain areas has been developed based on multitemporal data of ERS-1 SAR [6]. The temporal changes in σ° between the wet snow cover and reference images are utilized for the classification. As reference, SAR images for snow-free or dry snow conditions are used. Fig. 3 shows a flow chart of the snow classification algorithm. After calibration, the SAR images in slant range or ground range projection are co-registered and speckle filtered. The snow area is detected by means of a threshold of the σ° -ratio of the two images. The next step is terrain-corrected geocoding, for which a high accuracy digital elevation model is needed. In mountain areas steep slopes facing towards the radar antenna are strongly distorted; these are the foreshortening and layover zones, which can not be used for classification. In order to reduce the loss of information due to these effects, the SAR-derived snow cover maps from ascending and descending orbits are combined to derive a single map [6].

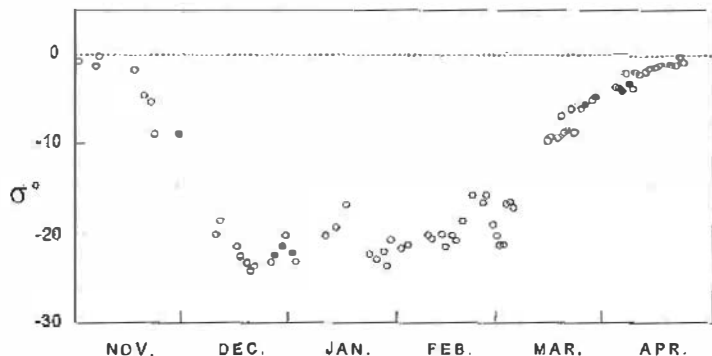


Fig. 2: Radar cross section σ° at 35° incidence angle, from ERS-1 scatterometer data, for the period 1 November 1992 to 25 April 1993 for a site at 76.5°S , 62.9°W on Larsen Ice Shelf, Antarctic Peninsula.

Simulated images are generated to assist in geocoding and to derive layover masks, shadow masks, and incidence angle maps. For generating the combined snow cover map from ascending and descending orbits, at first all pixels with local incidence angle $\theta \leq 15^{\circ}$ and $\theta \geq 80^{\circ}$ are excluded. Then the residual maps are combined under the rule that the pixel with the larger local incidence angle is selected if it is covered in both images. The accuracy of the algorithm was verified with

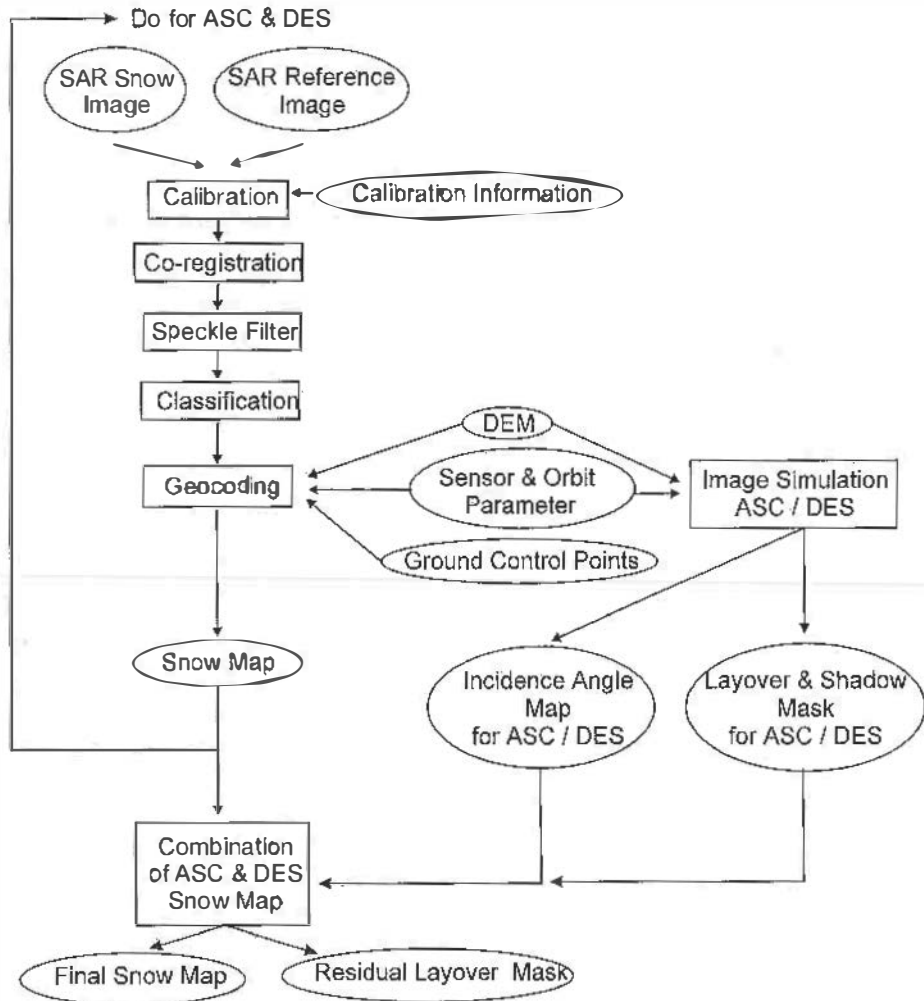


Fig. 3: Flow chart of the snow classification algorithm by means of spaceborne SAR. ASC - ascending, DES - descending orbit.

field data and with TM images of the test site Ötztal in the Central Alps of Tyrol. The comparisons indicated agreement for snow classifications of 80 % to 90 % on a pixel by pixel basis. The differences can be partly explained by time differences of several days between optical and SAR image acquisitions. The SAR-derived snow cover maps have already successfully been tested for modelling daily runoff due to snow and glacier melt [7, 8].

5. Climatic Response of Polar Ice and Glaciers Detected by ERS SAR

Dramatic changes of ice extent have been detected by means of ERS-1 SAR on the Antarctic

Peninsula and on the Southern Patagonian Icefield, providing evidence for changes in regional climatic conditions. The investigations on ice dynamics and ice/climate interactions in these regions are carried out in a joint research program of the Institut für Meteorologie und Geophysik der Universität Innsbruck and the Instituto Antártico Argentino, involving field campaigns and analysis of satellite data.

The Southern Patagonian Icefield, covering an area of about 13000 km² and stretching north-south for 350 km from 48.3°S to 51.5°S, is the largest ice-mass in the southern hemisphere north of Antarctica. Due to the extreme weather conditions with dense cloud cover and strong westerly winds throughout the year, knowledge

of the Patagonian glaciers is still very limited. Because of these conditions SAR is the optimum sensor for glacier research. Glaciological field work has been carried out at selected sites on Moreno Glacier (covering about 250 km² in area), Viedma Glacier (about 1000 km²), and Upsala Glacier (about 900 km²). Due to the size of the glaciers, remote sensing data are crucial for complementing the field measurements. ERS-1 SAR data were used to map glacier boundaries and ice flow features, to monitor changes of calving glacier fronts, and to study the temporal dynamics of accumulation and ablation zones. A major calving event in 1994 on Upsala Glacier, during which the glacier terminus retreated by 1.5 km, was documented by means of ERS-1 SAR [9].

Ice shelves make up about 40 % of the coastline of Antarctica. Because most of the ice that has accumulated over the grounded parts of Antarctica is discharged through the ice shelves, they play an important role in the mass budget and dynamics of the ice sheet. The ice shelves are floating masses of ice, with typical thickness of hundreds of meters, which are sustained by ice supply from grounded areas and in situ snowfall, in some regions also by basal freezing. Mass is lost due to calving of icebergs and due to basal melting. Surface melt is of importance only for the ice shelves at the Antarctic Peninsula. Ice shelves are particularly sensitive to climatic changes because they are exposed to both atmosphere and ocean.

A dramatic event of ice shelf disintegration was observed by means of ERS-1 SAR on northern Larsen Ice Shelf, which extends along the east coast of the Antarctic Peninsula [10]. In January 1995, within a few days, 4200 km² of the ice shelf broke away. The two northernmost sections of the ice shelf disappeared almost completely, the ice retreated to the grounding line. As an example, the section of the ice shelf between Sobral Peninsula and Larsen Nunatak is shown in Fig. 4. During the last five decades the ice front retreated slowly, coinciding with a trend of regional atmospheric warming. In summer 1992 the retreat accelerated. During a field campaign two month before the final disintegration an increased number

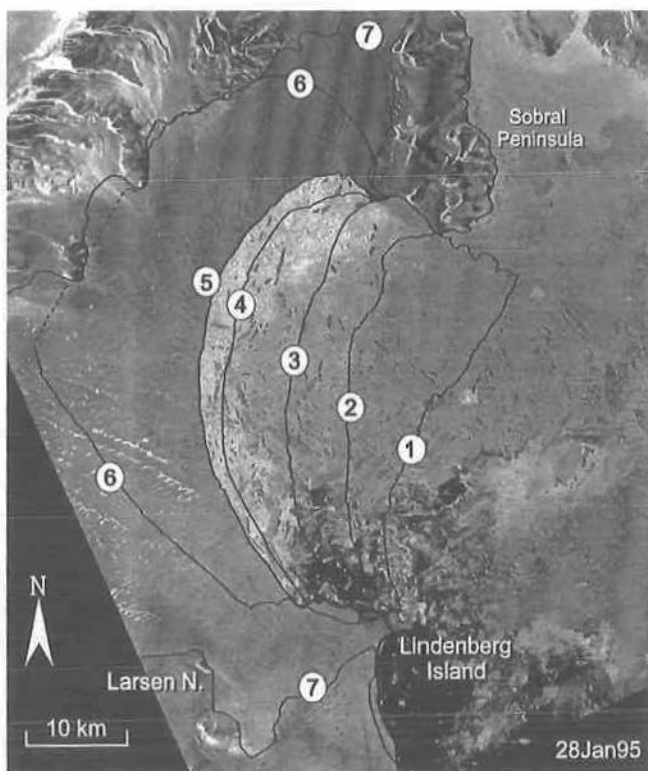


Fig. 4: ERS-1 SAR image of the Larsen Ice Shelf between Sobral Peninsula and Seal Nunataks, acquired on 28 January 1995. Ice front positions from ERS-1 SAR (2 to 6) and optical data (1 and 7). 1: 1 March 1986, 2: 8 December 1992, 3: 16 February 1993, 4: 25 January 1995, 5: 28 January 1995, 6: 30 January 1995, 7: 22 March 1995.

of crevasses and rifts indicated major changes in ice dynamics, but the rapidity of the collapse was not expected. The ice disintegrated finally in the form of comparatively small icebergs, some of these are visible in Fig. 4.

Mass balance considerations show that several hundred years would be needed to build up again the disintegrated sections of Larsen Ice Shelf. Under the present climatic conditions this seems not to be possible at all. The observations by means of ERS-1 shed new light on climate sensitivity and dynamics of ice shelves, indicating that ice shelves may collapse rapidly after retreat beyond a critical limit due to perturbations of the mass balance.

6. Further Methodological and Applications Research

Emphasis of methodological developments within ongoing research projects in Innsbruck are focusing on radar interferometry, based on

data from the ERS-1/ERS-2 Tandem Mission which were acquired over glaciers in the Alps, in Patagonia, and in Antarctica. The investigations are aiming at mapping of ice motion and topography. This information is required to understand the dynamic response of glaciers and ice sheets. During the Tandem Mission, between August 1995 and May 1996, the orbits have been adjusted so that ERS-2 SAR covers the same swath on the earth surface as ERS-1 with a time delay of 24 hours. Short repeat intervals are particularly important for cryospheric applications of interferometry, because the radar return of snow and ice is in general quite variable in time. The investigations by means of ERS are supplemented by an interferometric data set of the Spaceborne Imaging Radar C/X-Band Synthetic Aperture Radar (SIR-C/X-SAR) which was acquired over Moreno Glacier in Patagonia from the Space Shuttle Endeavour in October 1994 [11]. The interferograms of the X-, C-, and L-band data of SIR-C/X-SAR, acquired within 24 hours time difference, showed good coherence over the melting glacier only at L-band. The interferometrically derived velocities agree well with field measurements of ice velocity carried out at selected points. Whereas most parts of the glacier are inaccessible due to crevasses, the interferometric data provide information on ice motion over the whole glacier terminus revealing a complex pattern of ice dynamics not known before.

On the applied side, research is focusing on the use of SAR for snowmelt runoff modelling and forecasting. A sub-project of the research initiative „Multi-Image Synergistic Satellite Information for the Observation of Nature“ (MISSION) of the Austrian Science Ministry is aimed at the development of a model for calculating daily runoff using remote sensing data from SAR and optical sensors, as well as in situ measurements from automatic stations. Because regular repeat observations and spatially distributed data are important for operational hydrology, this is a

very promising field for operational applications of spaceborne SAR.

Acknowledgements

The research on methods and applications of SAR has been funded by the Austrian Academy of Sciences, National Space Research Program. The research activities related to Antarctica were supported by the Austrian Science Fund (FWF) Project P10709-GEO, logistic support was provided by the Instituto Antártico Argentino, Dirección Nacional del Antártico. The ERS data were made available by ESA for the ERS-1 Experiments AO.A1 and AO.A2 and for the ERS-2 Experiment AO2.A101.

References

- [1] Guyenne T.-D., Editor (1995) *New Views of the Earth, Scientific Achievements of ERS-1*. ESA SP-1176/1.
- [2] Rott H., K. Sturm, H. Miller (1993) Active and passive microwave signatures of Antarctic firn by means of field measurements and satellite data. *Annals of Glaciology* 17, 337-343.
- [3] Rott H. and Davis R.E. (1993) Multifrequency and polarimetric SAR observations on alpine glaciers. *Annals of Glaciology* 17, 98-104.
- [4] Rott H. and W. Rack (1995) Characterization of Antarctic firn by means of ERS-1 scatterometer measurements. *Proc. of IGARSS'95*, Firenze, July 1995, IEEE Cat. Nr. 95CH35770, 1747-1749.
- [5] Rack W. (1995) *Strukturverhalten und Morphologie der antarktischen Schneedecke aus Scatterometer-Messungen von ERS-1*. Diploma Thesis, Science Faculty, Univ. Innsbruck, 92 p.
- [6] Rott H. and T. Nagler (1994) Capabilities of ERS-1 SAR for snow and glacier monitoring in alpine areas. *Proc. of Second ERS-1 Symposium ESA SP-361*, 965-970.
- [7] Rott H. and T. Nagler (1995) Monitoring temporal dynamics of snowmelt with ERS-1 SAR. *Proc. IGARSS'95*, IEEE Cat. Nr. 95CH35770, 1747-1749.
- [8] Rott H., T. Nagler, D.-M. Florinčič (1996) Anwendungen der Fernerkundung für die Schneehydrologie. *Österr. Z. für Vermessung und Geoinformation*, 84. Jhg., 61-54.
- [9] Skvarca P., H. Rott, T. Nagler, (1995) Drastic retreat of Upsala Glacier, southern Patagonia, revealed by ERS-1/SAR images and field survey. *Revista SELPER* Vol. 11 (No. 1-2), 51-65.
- [10] Rott H., P. Skvarca, T. Nagler (1996) Rapid collapse of northern Larsen Ice Shelf, Antarctica. *Science*, Vol. 271, 788-792.
- [11] E.R. Stofan et al. (1995) Overview of results of Spaceborne Imaging Radar-C, X-Band Synthetic Aperture Radar (SIR-C/X-SAR). *IEEE Trans. Geosc. Rem. Sens.* 33, 817-828.

Anschrift der Autoren:

Dr. Helmut Rott, Thomas Nagler und Wolfgang Rack, Institut für Meteorologie und Geophysik, Universität Innsbruck, Innrain 52, A-6020 Innsbruck, Austria